VNU Journal of Science: Mathematics – Physics, Vol. 31, No. 1 (2015) 52-62

Optical Properties of Dy^{3+} and Ce^{3+} in Borate Glass

Tran Ngoc*

Quang Binh University, Vietnam

Received 19 December 2014
Revised 09 February 2015; Accepted 20 March 2015

Abstract: Spectroscopic properties of Dy^{3+} and Ce^{3+} ions doped alkali metal borate glasses (70-x-y)B_2O_3.15Li_2CO_3.15Na_2CO_3.xDy_2O_3 and yCeO_2 (BLN:Dy,Ce) fabricated by melting method have been studied. Energy transfer from the absorption and fluorescence center has been discussed. Judd–Ofelt (J-O) theory has been used to evaluate various spectroscopic properties such as oscillator strengths (f_{exp}, f_{cal}), intensity parameters $\Omega_\lambda(\lambda=2,4,6)$, spontaneous transition probabilities (A_R), radiative life times (τ_R) and luminescence branching ratios (σ_{exp}, σ_R). The cross-relaxation mechanism was discussed for BLN glass.

Keywords: Alkali metal borate glass, Energy transfer, cross-relaxation mechanism.

1. Introduction

Glasses doped with rare earth (RE) ions are good laser materials as they emit intense radiations in the visible (Vis), near-infrared (NIR) and infrared (IR) spectral regions under a suitable excitation conditions. Due to the unique structural and physico chemical properties, alkali metal borate glasses doped with RE ions have been widely used as laser materials, optical amplifiers, optical memories, optoelectronics and magneto-optical devices [10]. The presence of structurally different borate units in alkali metal borate glasses is favorable for spectroscopic investigations of RE ions. These structural differences are usually correlated to chemical composition, type of modifiers and conditions during glass preparation. Low phonon energy glasses doped with Dy^{3+} ions have been studied for optical amplifiers and yellow–green upconversion [11] applications. Special interest has been devoted to Dy^{3+} doped borate glasses with various chemical compositions [6]. Depending upon the host environment, the Dy^{3+} ions emit several emission bands between its f–f transitions [1]. The visible luminescence of the Dy^{3+} ion mainly consists of yellow band at 570–600 nm corresponding to the $^4F_{9/2}$-$^6H_{13/2}$ hypersensitive transition and the blue band at 470–500 nm corresponding to the $^4F_{9/2}$-$^6H_{15/2}$ transition. Dysprosium doped glasses and crystals emit intense discrete radiation in the yellow (570–600 nm) and NIR (1.35 and 3.0 mm) regions that have potential technological applications in commercial displays

* Tel.: 84-912098584
Email: daotaoqb@gmail.com

and telecommunications [6, 10]. The intensity of the $^4F_{9/2}$- $^6H_{13/2}$ hypersensitive transition strongly depends on the host, in contrast to a less sensitive $^4F_{9/2}$-$^6H_{15/2}$ transition of Dy^{3+} and results in different yellow to blue luminescence intensity ratios that largely change with concentration and/or glass composition.

In this works we prepared Dy^{3+} ions in alkali metal borate glasses and studied their spectroscopic properties. Judd–Ofelt (J-O) theory [3, 6] has been used to evaluate various spectroscopic properties such as oscillator strengths (f_{exp}, f_{cal}), intensity parameters $\Omega_\lambda(\lambda=2,4,6)$, spontaneous transition probabilities (A_R), radiative life times (τ_R) and luminescence branching ratios (σ_{exp}, σ_R). Energy transfer from the absorption and fluorescence center has been discussed. The cross-relaxation mechanism is also discussed for BLN glass.

2. Experiment

Alkali metal borate glass (BLN glass) doped RE^{3+} were prepared by conventional melt quenching technique. The molar composition of dysprosium doped BLN glasses investigated in this work is (68-x-y)B_2O_3-15Li_2O-15Na_2O-xDy_2O_3 and yCe_2O_3. The chemicals were weighed accurately in an electronic balance mixed thoroughly and ground to a fine powder. The batches were then placed in quartz cup and melted in an electrical furnace in air at 1323K for 1,5 hours. The melt was then quenched to room temperature in air by turning of the furnace. The glasses were then annealed at 650 K for 2 hours. The glasses thus obtained were throughout, evenly, no bubble. The samples were cutting, grinding, polishing blocks rounded product size: thickness d = 0.98 mm, radius r = 6.5 mm (used for the measurement of refractive index n, density, absorption and fluorescence); crushing and sorting grab particles range in size from 76 to 150 micron powder products (used for X-ray diffraction). The glass formation was confirmed by powder X-ray diffraction recorded.

The measurement of the refractive index n is made performed on the system Abbe refractometer at a wavelength of Nari, 589 nm with $C_{10}H_7Br$ (1- bromonaphthalin) used as the liquid in contact. The density measurements made by Archimede method, using xylene as immersion liquid form. Optical absorption spectra were recorded in the wavelength regions 200 nm – 2500nm using Varian spectrometer system cary 5E UV - VIS - NIR, with a resolution of 1nm. Fluorescence spectra were obtained at room temperature using Flourolog - 3 Model FL3 - 22, resolution of 0.3 nm, excitation light xenon (Vehicle).

3. Results and discussion

3.1. BLN: Dy^{3+} glass

1. Absorption spectra and Judd-Ofelt analysis

Room temperature absorption spectra of Dy^{3+} doped BLN glasses in the wavelength ranges 300nm - 500nm and 700nm - 1900 nm are shown in **Fig.1**(a,b).

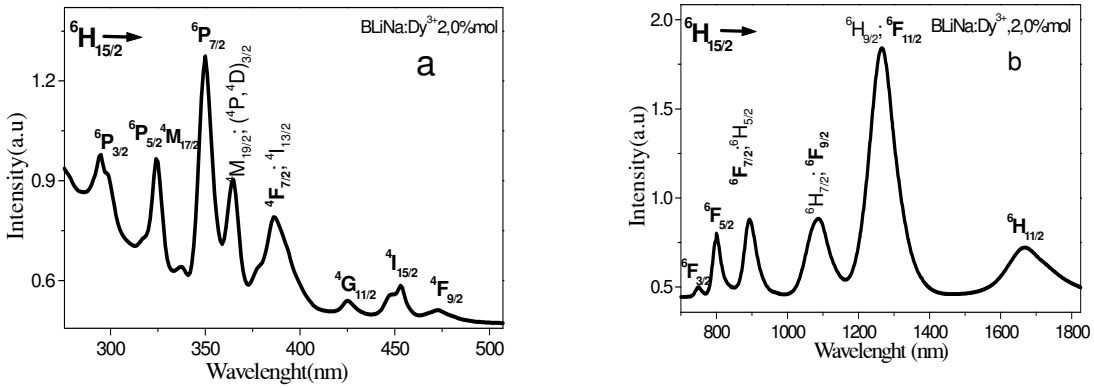

Fig. 1. The absorption spectra of BNaLi glass doped with 2.0 mol% of Dy^{3+} ions in range 300 -500 nm (a) and 700 -1900 nm (b).

The intensities of absorption bands are measured in terms of experimental oscillator strengths (f_{exp}) determined from the relative areas under the absorption bands. For J-O analysis, the f_{exp} values of sevent observed absorption bands at 320, 350, 362, 381, 425, 455 and 470 nm (in the wavelength range 300nm - 500nm) and six observed absorption bands at 745, 800, 895, 1090, 1270 and 1675 nm (in the wavelength range 700nm - 1900nm) which are assigned at different transitions from the $^6H_{15/2}$ ground state to the, $^6P_{3/2}$,$^4M_{17/2}$, $^6P_{7/2}$, $^4M_{19/2}$,$^4(D,P)_{3/2}$,$^6P_{3/2}$, $^4F_{7/2}$, $^4I_{13/2}$, $^4G_{11/2}$ $^4I_{15/2}$, $^4F_{9/2}$ and $^6F_{3/2}$,$^6F_{5/2}$,$^6F_{7/2}$,$^6H_{7/2}$, $^6H_{9/2,}$ $^6F_{11/2}$, $^6H_{11/2}$ excited states, respectively, are taken into account [2,7,9]. Using the squared reduced matrix elements $\|U^{(\lambda)}\|^2$ and the experimental oscillations (f_{exp}), the calculated oscillator strengths (f_{cal}) as well as the three J–O intensity parameters $\Omega_\lambda(\lambda=2,4,6)$ are determined by a least square fit method using the following equation [3,6]:

$$f_{cal}(\psi J,\psi' J') = \frac{8\pi^2 mc\upsilon}{3h(2J+1)} \frac{(n^2+2)^2}{9n} \sum_{\lambda=2,4,6} \Omega_\lambda \left\langle \psi J \left\| U^{(\lambda)} \right\| \psi' J' \right\rangle^2$$

where m is the mass of an electron, c is the speed of light, h is the Plank's constant, n is the refractive index of the sample and J is the total angular momentum quantum number. The factor (2J+1) represents the degeneracy of the ground state, i.e. The terms S_{ed} and S_{md} are the electric and magnetic dipole line strengths, respectively. The reduced matrix elements $\|U^{(\lambda)}\|^2$, which are insensitive to the ion environment, were taken from the literature [2]. Table 1 presents the wavelengths of absorption bands, experimental and calculated oscillator strengths of the studied glasses.

Table 1. Energy flow of absorption bands and experimental (f_{exp}) and calculated (f_{cal}) oscillator strengths of Dy^{3+}doped BLN glass.

Transition from $^6H_{15/2}$ to	E_{exp} (cm^{-1})	E_{quo} (cm^{-1})	f_{exp} ($\times10^{-6}$)	f_{cal} ($\times10^{-6}$)
$^6H_{11/2}$	5995	5850	3.21	3.07
$^6F_{11/2}$,$^6H_{9/2}$	7898	7730	16,54	16,57
$^6F_{9/2}$,$^6H_{7/2}$	9199	9100	5.97	6,50

$^6F_{7/2}$	11198	11000	4.91	5,15
$^6F_{5/2}$	12468	12400	3.25	2,36
$^6F_{3/2}$	13351	13250	0.39	0,48
$^4F_{9/2}$	21141	21100	0.54	0,39
$^4I_{15/2}$	22075	22100	1.18	1,04
$^4G_{11/2}$	23529	23400	0.29	0,21
$^4F_{7/2}$,$^4I_{13/2}$	25839	25800	4.45	1,91
$^4M_{19/2}$,$^4(D,P)_{3/2}$,$^6P_{3/2}$	27397	27400	3.90	3,50
$^6P_{7/2}$	28571	28550	9.12	7,89
$^6P_{3/2}$,$^4M_{17/2}$	30864	30892	3.14	2,02
			rms = $1,09\times10^{-6}$	

The bonding parameter (δ) depends on the environmentel fied, δ can be received the positive or negative value indicating covalent or ionic bonding. In our sample, the value of δ bonding parameter are -1.63, thus in this case the bonding of Dy^{3+} ions with the local host is ionic bonding [4,10]. The evaluated JO intensity parameters are compared with those reported for different Dy^{3+} doped glasses [7,8,9,11] as presented in Table 2.

Table 2. The JO parameters of Dy^{3+} ions doped various hosts

Host matrix	Ω_2(x10^{-20}cm^2)	Ω_4(x10^{-20}cm^2)	Ω_4x10^{-20}cm^2)	Ref.
BLNa: Dy glass	16,28	5,78	5.32	Present
LiLTB: Dy glass	8,75	2,62	2,07	[7]
NLTB: Dy glass	9,25	2,87	2,29	[7]
NLTB: Dy glass	9,86	3,39	2,41	[7]
LB: Dy glass	12,83	3,47	3,43	[8]
PKMAF:Dy glass	7,04	1,73	1,57	[9]
PKBFA:Dy glass	10,41	2,29	2,07	[11]

In the present work, the intensity parameters follow the trend as $\Omega_2 > \Omega_4 > \Omega_6$ in glasses. In general, the J-O parameters provide an insight into the local structure and bonding in the neighbourhood of RE^{3+} ions. In particular, magnitude of structure/environment parameter Ω_2 depends on covalency of metal ligand bond and also explains the symmetry in the vicinity of RE ion sites. The Ω_2 parameter characterizing the asymmetry of the coordination structure, the polarization of the ligand and the nature of the link between the Dy^{3+} ions with other ions (O^- , Li ..). The higher magnitude of Ω_2 suggests that the Dy^{3+} ion site has lower asymmetry in BLiNa glasses (polarization is large). The Ω_4 parameter is related to the bulk properties and Ω_6 is inversely related to the rigidity of host [11,12]. The spectroscopic quality factor $X=\Omega_4/\Omega_6$ (=1,14) is one of the important lasing characteristic parameters which is used to predict the stimulated emission in any active medium. The Dy^{3+}doped glass hosts possessing spectroscopic quality factors in the range 0.42–1.92 are the good candidates for laser active media [11, 13].

2. Excitation spectra. In order to investigate the luminescen ce properties as a function of Dy^{3+} ion concentration, the excitation spectra were recorded in the spectral region 300–500 nm by monitoring the emission at 577 nm ($^4F_{9/2}$ - $^6H_{13/2}$). Fig.2 shows the excitation spectrum of 2.0 mol% Dy^{3+} doped BLN glass along with the assignment of band positions. The excitation bands centered at 325; 350;

365; 387; 425; 453 and 475 nm correspond ing to $^6H_{15/2} \rightarrow {}^6P3/2;{}^6P_{7/2}$; $^4P_{3/2}$; $^4F_{7/2}$; $^4G_{11/2}$, $^4I_{15/2}$ and $^4F_{9/2}$, transitions, respectively.It is a well known fact that the wavelength corresponding to the prominent excitation band can give intense emission . In the present investiga tion, the excitation band centered at 454 nm is found to be more intense. Thus, the luminescen ce spectra were carried out by exciting the samples with 454 nm wavelength.

3. Fluorescence spectra and radiation characteristic displacement

Fluorescence spectra measured in the wavelength ranges from 400nm to 750nm of Dy^{3+} in the BLN glass at temperature room shown in **Fig. 3**

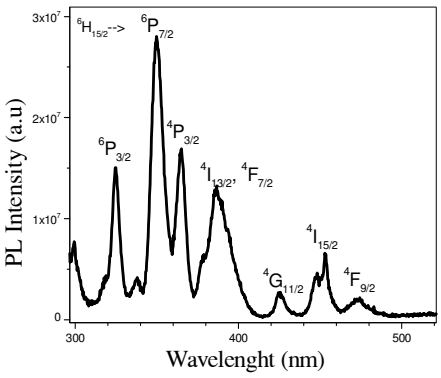

Fig 2. Excitation spectra of 2.0 mol% of Dy^{3+}doped BLiNa glasses

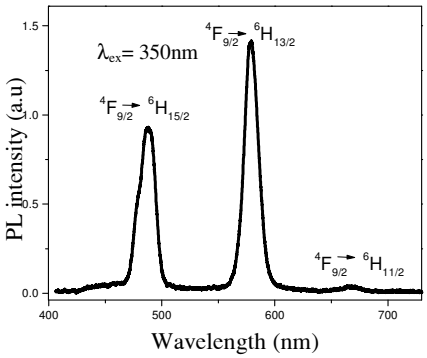

Fig 3. PL spectrum of Dy^{3+} in the BLN glass.

It exhibits four emission bands observed at the position 454nm, 478 nm, 585 nm and 668 nm which are assigned from high-level stimulus $^4I_{15/2} \rightarrow {}^6H_{15/2}$ and $^4F_{9/2} \rightarrow {}^6H_{15/2}$, $^6H_{13/2}$ and $^6H_{11/2}$ transitions, respectively [7, 8, 9, 10]. The violet (454 nm) and red (668 nm) emissions are very feeble, while the blue (478 nm) and yellow (585 nm) emissions are more intense. Emission peak positions (λ_p), effective line width ($\Delta\lambda_{eff}$), radiative transition probabilities (A), branching ratios (β_{exp}), stimulated emission cross – section $\sigma(\lambda_P)$ and integrated emission cross – section (Σ_{if}) for $^4F_{9/2} \rightarrow {}^6H_J$ transitions of Dy^{3+} displayed in the **table 3.**

Table 3. Emission peak positions (λ_p), effective line width ($\Delta\lambda_{eff}$), radiative transition probabilities (A), branching ratios (β_{exp}), stimulated emission cross – section $\sigma(\lambda_P)$ and integrated emission cross – section (Σ_{if}) for $^4F_{9/2} \rightarrow {}^6H_J$ transitions of Dy^{3+} in BLN glass.

$^4F_{9/2} \rightarrow$	λ_p (nm)	$\Delta\lambda_{eff}$ (nm)	A (s^{-1})	$\sigma(\lambda_p)$ ($\times 10^{-22}$ cm^2)	Σ_{if} ($\times 10^{-18}$ cm)	β_R (%) exp	cal
$^6H_{11/2}$	662.3	25.9	159	6,5	0.38	4,6	6,59
$^6H_{13/2}$	574.7	16.4	1620	60,1	2.99	54,8	66,9
$^6H_{15/2}$	481.4	18.5	448	7,2	0.58	40,6	18,5

The radiative properties such as transition energies (ν), radiative transition probabilities (S_{ed}, S_{md}, A and A_T), radiative lifetime (τ_R) and branching ratios (β_R) for excited levels are evaluated using the Judd-Ofelt theory, results displayed in the **table 4.**

Table 4. Transition energies (ν), radiative transition probabilities (S_{ed}, S_{md}, A and A_T), radiative lifetime (τ_R) and branching ratios (β_R) for excited levels.

SLJ	*S'L'J'*	*v* (cm^{-1})	S_{ed} (cm^2)	S_{md} (cm^2)	*A* (s^{-1})	β_R (%)
$^4F_{9/2}$	$^6F_{1/2}$	7,291	4.90E-42	0.00E+00	1.94E-01	8.01E-03
	$^6F_{3/2}$	7,902	4.00E-42	0.00E+00	1.97E-01	8.16E-03
	$^6F_{5/2}$	8,556	2.59E-40	0.00E+00	1.71E+01	7.09E-01
	$^6F_{7/2}$	9,946	1.03E-40	4.00E-41	1.13E+01	4.67E-01
	$^6H_{5/2}$	10,900	6.13E-41	0.00E+00	8.11E+00	3.35E-01
	$^6H_{7/2}$	11,963	2.30E-40	1.76E-41	4.06E+01	1.68E+00
	$^6F_{9/2}$	12,066	1.07E-40	1.59E-41	1.94E+01	8.01E-01
	$^6F_{11/2}$	13,258	2.09E-40	2.26E-42	5.10E+01	2.11E+00
	$^6H_{9/2}$	13,398	1.61E-40	1.65E-40	4.46E+01	1.84E+00
	$^6H_{11/2}$	15,209	4.34E-40	3.13E-41	1.59E+02	6.59E+00
	$^6H_{13/2}$	17,628	2.89E-39	0.00E+00	1.62E+03	6.69E+01
	$^6H_{15/2}$	21,182	4.64E-40	0.00E+00	4.48E+02	1.85E+01
$A_T(^4F_{9/2}) = 2420\ s^{-1}$; $\tau_R(^4F_{9/2}) = 413\ \mu s$						

Analysis the tables (2 and 3) shows: at a particular yellow to blue (Y/B) intensity ratio of ($^6F_{9/2}\rightarrow{}^6H_{13/2}/{}^6F_{9/2}\rightarrow{}^6H_{15/2}$) emission transitions, the Dy^{3+} ions will emit white light. In the present study, the evaluated (Y/B) ratios are 1,6 for BLN: Dy glasses. Nephelauxetic ratio β_R and emission cross section σ greatest value to the displacement $^4F_{9/2} \rightarrow {}^6H_{13/2}$, followed by $^4F_{9/2} \rightarrow {}^6H_{15/2}$. Such displacement of concern here is $^4F_{9/2} \rightarrow {}^6H_{13/2}$ is β_R and σ large ($60{,}1\times10^{-22}$ cm^2), the evaluated emission cross-sections suggest that the BLN:Dy glasses are more useful for the generation of yellow luminescence [7,11].

4. Cross – Relaxation channels

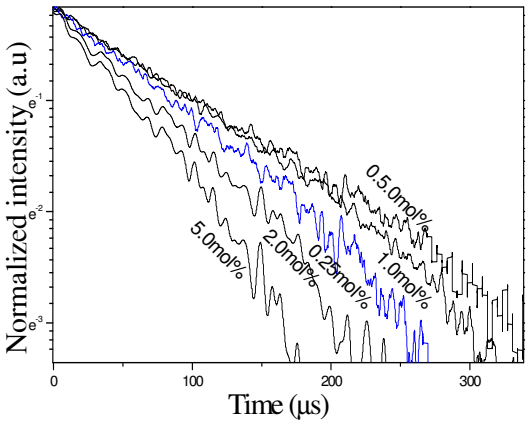

Fig 4. Decay curves in BLN glasses for different Dy^{3+} ion concentrations.

Fig. 4 presents the experimental decay curves obtained for different Dy^{3+} ion concentrations. The lifetimes of the $^4F_{9/2}$ level have been determined and were showed in **table 5.** The decay profiles of $^4F_{9/2}$ emission level of Dy^{3+} ions in LBZLFB glass containing different concentrations of Dy^{3+} ions were recorded under excitation at 350 nm and emission at 577 nm. It is observed that, the decay profiles are found to be single exponenti al for lower concentrations, i.e., for 0.25 and 0.5 mol% and for higher concentr ations (1.0, 2.0 and 5.0 mol%) of Dy^{3+} ions the decay curves deviate towards non-exponential nature.

Table 5. Variation of lifetime with respect to concentration (%) of Dy^{3+} ions in BLN glasses

Concentration (**%Dy**)	Lifetime τ_m (**µs**)
BLN: 0,25 Dy %mol	280
BLN: 0,5 Dy %mol	380
BLN: 1,0 Dy %mol	347
BLN: 2,0 Dy %mol	260
BLN: 5,0 Dy %mol	195

From the decay curves, lifetime (τ_m) of the $^4F_{9/2}$ level has been determined by taking the first efolding time of the decay intensity. The measured decay time (τ_m) of the $^4F_{9/2}$ emission state is found to be **table 5**. The fluorescence lifetime at lower concentr ations is close to the radiative lifetime (τ_m); however as the concentration increases, the lifetime decreases which indicates the presence of non-radiative energy transfer processes from excited state to neighboring unexcited state of Dy^{3+} ions. The discrepancy between the measured and calculated lifetimes is mainly due to energy transfer through cross-relaxation or multi phonon relaxation or both. The measured lifetime (τ_m) of an emitting state is related with the radiative lifetime (τ_R) and non-radiative decay rates as $\tau_m < \tau_R$.

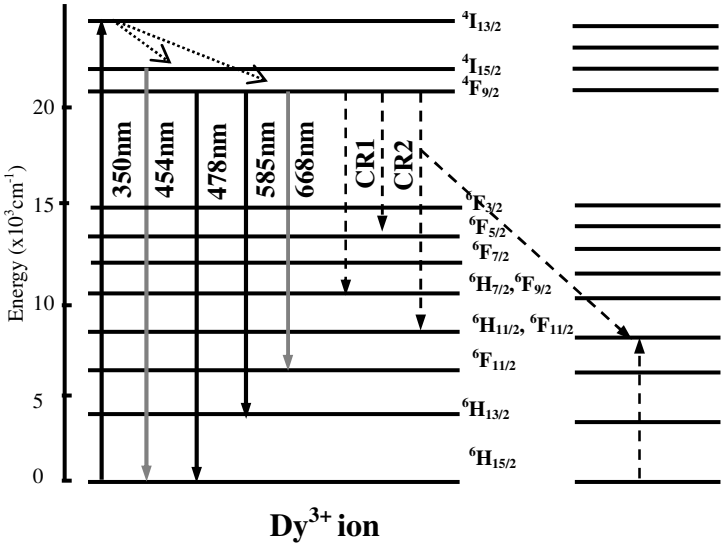

Fig.5. Partial energy level diagram showing the energy transfer cross-relaxation channels of Dy^{3+} ions in BLN glasses.

From the absorption and emission spectra of BLN: Dy^{3+} glasses, the energy level diagram of Dy^{3+} in BLN glass and was shown in **Fig 5.** When Dy^{3+} ions are excited to the higher levels of the $^4F_{9/2}$, there is a fast non-radiative relaxation to this fluorescent level and emission takes place from $^4F_{9/2}$ level to its lower levels. The energy transfer process through cross – relaxation (CR) between the pair Dy^{3+} ions (as shown in Fig.5 leads luminescence quenching. The cross – relaxation channels in BLN glasses may be estimated to be: $^4F_{9/2}+{}^6H_{15/2}\rightarrow{}^6H_{5/2}+{}^6H_{7/2}$ (CR1) and $^4F_{9/2}+{}^6H_{15/2}\rightarrow{}^6F_{3/2}+{}^6H_{9/2}$(CR2) as the energy difference between these transitions are negligible [11]. The cross-relaxation is due to the energy transfer from the Dy^{3+} ion in an excited $^4F_{9/2}$ state to a near Dy^{3+} ion in the ground state $^6H_{15/2}$ state. This transfer leads the first ion in the intermediate level of $^6H_{9/2}$ (or $^6F_{3/2}$) and the second one in $^6H_{7/2}$ (or $^6F_{5/2}$), which occur in resonance with the $^4F_{9/2}\rightarrow{}^6H_{9/2}$ (or $^4F_{9/2}\rightarrow{}^6H_{7/2}$) transition. Then, from these states, the Dy^{3+} ions will relax to ground state by non-radiative relaxation. Thus, emission will be quenched. These cross-relaxation channels are indicated in the partial energy level diagram of Fig.5 by the dotted arrows as CR1 and CR2, respectively [3, 5, 6].

3.2. BLN: Ce^{3+} glass

1. Absorption spectra: Room temperature absorption spectra of Ce^{3+} doped BLN glasses in the wavelength ranges 240nm - 400nm are shown in **Fig. 6**. With intense absorption bands in the UV region and originate from the ground state $^2F_{5/2}$ to the various higher states (absorption spectrum is broad band characteristic for the transition 4f-5d). Unlike other rare earth elements, the optical process of Ce ion depends greatly on the lattice so the overall network expansion of distance depending crystal field around Ce^{3+} ions [1,3].

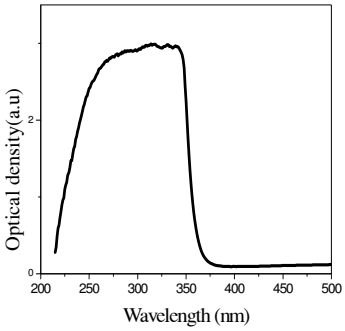

Fig.6. Absorption spectra of Ce^{3+}doped BLN glasses.

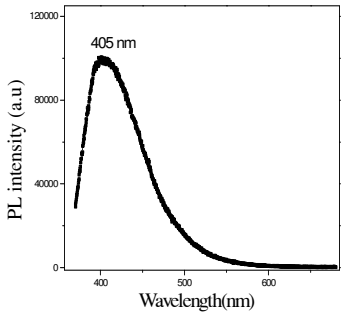

Fig.7. Fluorescence spectra of Ce^{3+}doped BLN glasses.

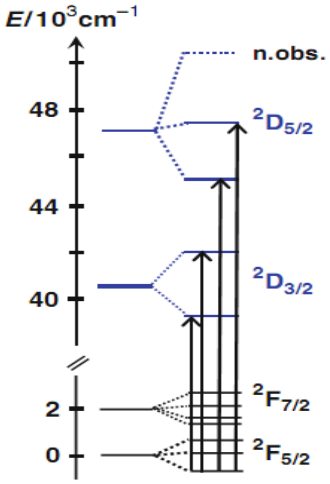

Fig.8. Assignment (D_{3h} symmetry).

2. Fluorescence spectra: Fluorescence spectra of Ce^{3+} doped BLN glass were measured in the wavelength range from 350 nm to 670 nm at temperature room shown in Fig. 7. Broad band emission with maximum at 405 nm (violet luminescence) characteristic of displacement 4f-5d. The 4f–5d

transitions have high energies of Ce^{3+} ion are commonly observed. Figure 8 shows the crystal-field splitting of both the $4f^1$ ($^2F_{5/2}$, $^2F_{7/2}$) and $5d^1$ ($^2D_{3/2}$, $^2D_{5/2}$) electronic configurations of Ce^{3+} in D_{3h} symmetry. In the displayed spectrum, the third transition to $^2D_{5/2}$ is not observed because it lies at too high energy. Conversely, the Ce^{3+} luminescence can be tuned from about 300 to 500 nm, depending on the matrix into which the metal ion is inserted, because of large crystal-field effect on the $5d^1$ excited state [1, 3].

3.3. BLN: Dy^{3+}, Ce^{3+} glass

1. Absorption spectra: Room temperature absorption spectra of Dy^{3+}, Ce^{3+} doped BLN glasses in the wavelength ranges 240nm - 2000nm are shown in **Fig.10.** Absorption spectrum is the sum of the absorption of Dy^{3+} (fig1) and Ce^{3+} (fig7). Intense absorption bands locate in the UV (240nm - 400nm) region (absorption of Ce^{3+}). Originate from the ground state to the various higher states (absorption spectrum is broad band characteristic for the transition $4f^1(^2F_{5/2})$ to the various higher states $5d^1(^2D_{3/2}$, $^2D_{5/2})$. Unlike other rare earth elements, the optical process of Ce^{3+} depends greatly on the matrix so the overall network expansion of distance depending 4f-5d crystal field around Ce^{3+} ions [1,3].

The compatibility of the two spectra in the range 400 nm to 2000 nm shows absolutely no Ce^3 ions absorb photons in this region. All the transitions in the absorption spectrum of Dy^{3+} are intra-configuration (f-f) transitions and originate from the ground state $^6H_{15/2}$ to higher energy states (^6P_J, ^4M_J $^4(D,P)_J$, ^4F_J, ^4I_J, ^4G_J, ^6F_J and $^6H_{7/2}$) [2,7,9].

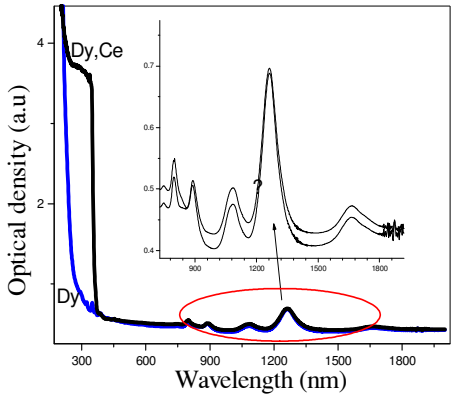

Fig 10. Absorption spectra of Dy^{3+} and Dy^{3+}, Ce^{3+} doped BLN glasses.

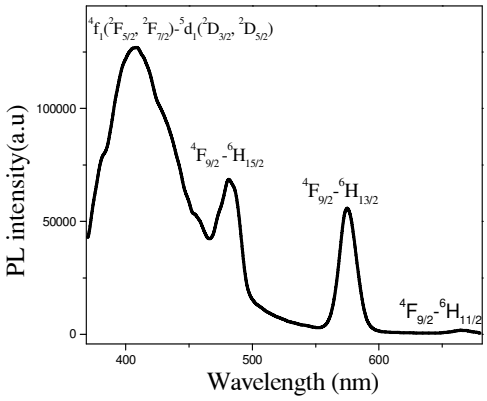

Fig 11. Fluorescence spectra of Dy^{3+}, Ce^{3+} doped BLN glasses.

2. Fluorescence spectra: **Fig.11** presents the emission spectrum of Dy^{3+}, Ce^{3+} doped BLN glasses. Broad band fluorescence (300 nm - 500 nm) with maximum at 405 nm (violet luminescence) that characterizes for displacement 4f-5d. The 4f–5d transitions have high energies and only those of Ce^{3+} are commonly observed $4f^1(^2F_{5/2}$, $^2F_{7/2})$ and $5d^1(^2D_{3/2}$, $^2D_{5/2})$ electronic configuration of Ce^{3+} in D_{3h} symmetry [1,3].

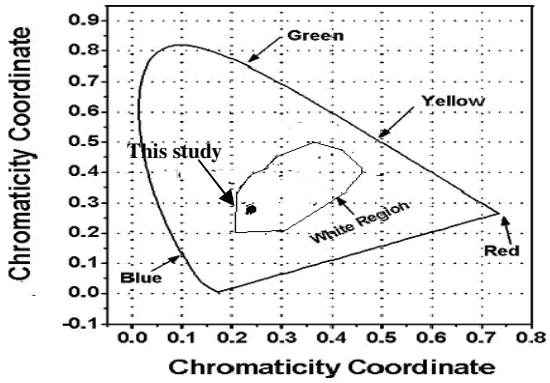

Fig.12. Chromaticity diagram of BLN glasses doped with Dy^{3+}, Ce^{3+} ions.

The emission spectrum of Dy^{3+} ions in the wavelength ranges from 400nm to 750nm, It exhibits four emission bands observed: The violet (454 nm) and red (668 nm) emissions are very feeble, while the blue (478 nm) and yellow (585nm) emissions are more intense. Among these three transitions, the $^4F_{9/2} \rightarrow {}^6H_{15/2}$ (blue) is magnetic dipole (MD) transition possessing higher intensity, $^4F_{9/2} \rightarrow {}^6H_{11/2}$ (red) possessing lower intensity and $^4F_{9/2} \rightarrow {}^6H_{13/2}$ (yellow) transition possessing moderate intensity related to the electric dipole (ED) transition [6,7]. The location of chromaticity coordinates (x= 0,237, y= 0,295) are shown in the inset **Fig.12** for the BLN: Dy^{3+}, Ce^{3+} glasses. From these results it is noticed that the chromaticity coordinates of BLN glasses doped with Dy^{3+}, Ce^{3+} ions are located in the white light region of CIE chromaticity diagram.

4. Conclusion

Dy^{3+} doped BLN glasses were prepared by melt quenching technique and investigated through the optical absorption and photoluminescence. Judd–Ofelt theory has been applied to determine the intensity parameters Ω_λ (λ=2,4,6) follow the trend as $\Omega_2 > \Omega_4 > \Omega_6$ in all the BLN glasses. The Ω_2 parameter characterizing the asymmetry of the coordination structure, the polarization of the ligand and the nature of the link between the Dy^{3+} ions with other ions (O, Li, Na...). The higher magnitude of Ω_2 suggests that the Dy^{3+} ion site has lower asymmetry in BLN glasses (polarization is large). Several radiative and laser characteristic parameters have been evaluated using the J–O intensity parameters and emission measurements. The luminescence spectra show two intense bands at 478 nm, 585 nm, which are attributed to $^4F_{9/2} \rightarrow {}^6H_{15/2}$ (blue) and $^4F_{9/2} \rightarrow {}^6H_{13/2}$ (yellow) transitions, respectively.

The cross-relaxation mechanism is also discussed for BLN glass. The cross – relaxation is due to the energy transfer from the Dy^{3+} ion in an excited $^4F_{9/2}$ state to a near Dy^{3+} ion in the ground state $^6H_{15/2}$ state. This transfer leads the first ion in the intermediate level of $^6H_{9/2}$ (or $^6F_{3/2}$) and the second one in $^6H_{7/2}$ (or $^6F_{5/2}$), which occur in resonance with the $^4F_{9/2} \rightarrow {}^6H_{9/2}$ (or $^4F_{9/2} \rightarrow {}^6H_{7/2}$) transition. Then, from these states, the Dy^{3+} ions will relax to ground state by nonradiative relaxation. Thus, emission will be quenched.

In the absorption spectra of Dy^{3+} and Ce^{3+} ions doped BLN glasses, the intense absorption bands locate in the UV (240nm - 400nm) region absorption of Ce^{3+} that originate from the ground state to the various higher states. Absorption bands in the Vis and IR (400nm-2000nm) region ascribe to absorption of Dy^{3+}. All the transitions in the absorption spectrum of Dy^{3+} are intra-configurational (f-f) transitions and originate from the ground state $^6H_{15/2}$ to higher energy states.

Broad band fluorescence (300nm-500nm) with maximum at 405 nm (violet luminescence) characterize the displacement 4f-5d. The 4f–5d transitions have high energies and only those of $Ce^{3+}$are commonly observed ($4f^1$ ($^2F_{5/2}$, $^2F_{7/2}$) and $5d^1$ ($^2D_{3/2}$, $^2D_{5/2}$) electronic configurations of Ce^{3+} in D_{3h} symmetry.

References

[1] Christane Görller, Walrand and K. Binnemans, Handbook on the Physics and Chemistry of Rare Earths. Vol.25, pp 101 – 252.
[2] Carnall W.T., Fields P.R., and Rajnak K, J. Chem. Phys, Vol. 49, No 10, (1968), pp. 4424-4442.
[3] Judd BR, Phy Rev (1962),127:750–61.
[4] Jørgensen CK, Reisfeld R, J Less-Common Met. (1983), 93:pp.107–120.
[5] Lin H, Pun EYB, Wang X, Lin X, J Alloys Compd, (2005), 390:pp.197–201.
[6] Ofelt GS, J Chem Phys (1962), 37:511–20 “fluoroborate glasses”, Opt Mater (2000), 15: pp. 65–79.
[7] S.A. Saleema, B.C. Jamalaiah, M. Jayasimhadri, A. Srinivasa Rao,Kiwan Jang, L. Rama Moorthy; Journal of Quantitative Spectroscopy & Radiative Transfer (2011), pp.78–84.
[8] Surendra Babu S, Babu P, Jayasankar CK, Siewers W, Wortmann G, Opt. Mater, (2009), 31:624–31.
[9] Sardar DK, Bradley WM, Yow RM, Gruber JB, Zandi B, J Lumin , (2004), 106:pp.195–203.
[10] Tripathi G, Rai VK, Rai SB, Spectrochim Acta A, (2005);62:1120–4.
[11] Tanabe S, Kang J, Hanada T, Soga N, J. Non-Cryst Solids, (1998);239:170–5.
[12] Yang Z, Li B, He F, Luo L, Chen W, J Non-Cryst Solids , (2008);354:1198–200.